Biochimica et Biophysica Acta 1818 (2012) 2550–2562

Contents lists available at SciVerse ScienceDirect

Biochimica et Biophysica Acta

journal homepage: www.elsevier.com/locate/bbamem

Review

Role of lipid ordered/disordered phase coexistence in pulmonary surfactant function

Cristina Casals *, Olga Cañadas

Departamento de Bioquímica y Biología Molecular I & CIBER de Enfermedades Respiratorias, Universidad Complutense de Madrid, 28040, Madrid, Spain

ARTICLE INFO

Article history:
Received 5 January 2012
Received in revised form 3 May 2012
Accepted 22 May 2012
Available online 31 May 2012

Keywords:
Lateral phase separation
SP-A
SP-B
SP-C
Surface activity
Surfactant inhibition

ABSTRACT

The respiratory epithelium has evolved to produce a complicated network of extracellular membranes that are essential for breathing and, ultimately, survival. Surfactant membranes form a stable monolayer at the air–liquid interface with bilayer structures attached to it. By reducing the surface tension at the air–liquid interface, surfactant stabilizes the lung against collapse and facilitates inflation. The special composition of surfactant membranes results in the coexistence of two distinct micrometer-sized ordered/disordered phases maintained up to physiological temperatures. Phase coexistence might facilitate monolayer folding to form three-dimensional structures during exhalation and hence allow the film to attain minimal surface tension. These folded structures may act as a membrane reserve and attenuate the increase in membrane tension during inspiration. The present review summarizes what is known of ordered/disordered lipid phase coexistence in lung surfactant, paying attention to the possible role played by domain boundaries in the monolayer-to-multilayer transition, and the correlations of biophysical inactivation of pulmonary surfactant with alterations in phase coexistence.

Contents

1. Introduction

To facilitate gas exchange, the lung has the largest epithelial surface area of the body in contact with the external environment. Our current understanding of the alveolus includes (Fig. 1): type I epithelial cells that mediate gas exchange; type II epithelial cells that produce and secrete lung surfactant and, in addition, have proliferative and innate immune functions; endothelial cells with critical gas exchange and metabolic functions; alveolar macrophages that coordinate host defense; and interstitial fibroblasts that support alveolar structure through the secretion of extracellular matrix proteins [1]. In addition, epithelial cells and alveolar macrophages are covered by a layer of aqueous fluid that contains extracellular membranes called pulmonary surfactant (Fig. 1). Surfactant is necessary to keep the alveolus open, thereby allowing gas exchange. Without surfactant the alveoli collapse since the surface tension at the air–water interface exerts a collapsing pressure. Thus, one of the main lung surfactant functions is to form a stable lipid monolayer at the air–liquid interface that excludes water molecules from the interface and effectively lowers surface tension to almost 0 mN/m on expiration [2–6].

Abbreviations: AFM, atomic force microscopy; DPPC, dipalmitoylphosphatidylcholine; L_d, liquid-crystalline disordered; L_o, liquid-crystalline ordered; LE, liquid expanded; LO, liquid expanded ordered; TC, tilted condensed; PL, Phospholipid; PC, phosphatidylcholine; ToF-SIMS, time-of-flight secondary ion mass spectroscopy; γ, surface tension; γ_e, equilibrium surface tension; π, surface pressure; π_e, equilibrium surface pressure

* Corresponding author at: Department of Biochemistry and Molecular Biology I, Faculty of Biology, Complutense University of Madrid, 28040 Madrid, Spain. Tel.: +34 91 3944261; fax: +34 91 3944672.
E-mail address: ccasalsc@bio.ucm.es (C. Casals).
URL: http://www.ucm.es/info/respira/ (C. Casals).

0005-2736/$ – see front matter © 2012 Elsevier B.V. All rights reserved.
doi:10.1016/j.bbamem.2012.05.024

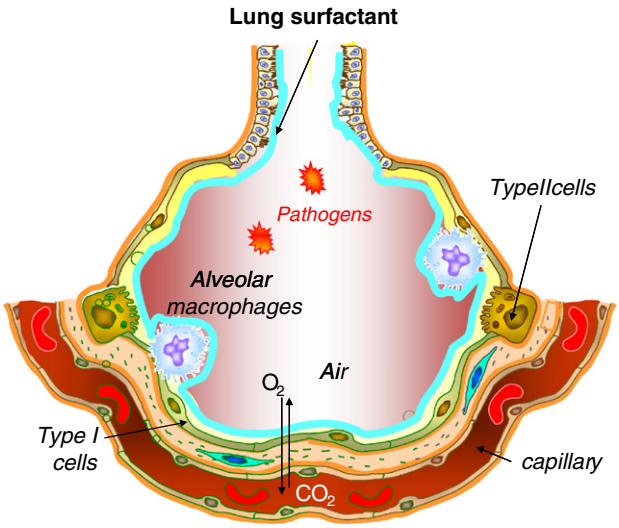

Fig. 1. The alveoli are composed of a thin alveolar epithelium composed of two cell types: thin, squamous type I cells, which cover 95% of the alveolar surface and form the structure of the alveolar wall, and cuboidal type II cells that secrete pulmonary surfactant. Alveoli also contain macrophages that are involved in lung defense. The alveolar epithelial cells and alveolar macrophages are covered by a layer of aqueous fluid that contains extracellular membranes called pulmonary surfactant.

Lung surfactant not only protects the lung against alveolar collapse and facilitates inflation on inspiration, but, together with alveolar macrophages, constitutes the front line of defense against inhaled pathogens and toxins. These two essential surfactant functions—lowering surface tension and host defense—depend on the complexity of the lipid and protein constituents of the surfactant system [7–10]. It is thought that these two functions are inseparably coordinated so that host defense mechanisms at the interface do not interfere with the surface-active properties of the surfactant system.

Lung immaturity and surfactant deficiency are the main factors in the pathogenesis of neonatal respiratory distress syndrome (RDS) [10,11]. In addition, surfactant dysfunction, caused by inactivation of surface-active material in the airspaces, contributes to respiratory failure in other forms of neonatal or adult lung diseases [4,8,10–12]. Airway instillation of surfactant is in general use for treatment of RDS in preterm babies [11]. Animal-derived replacement surfactants consist of lipid extract preparations obtained from animal bronchoalveolar fluids [11]. Unfortunately, commercial animal-derived replacement surfactants have inferior surface activity and are more susceptible to inactivation than native surfactants, possibly as a consequence of their reduced SP-B/C content, the lack of SP-A, and (with the exception of Survanta) higher fractions of unsaturated phospholipid species than natural surfactant [13]. A better comprehension of structure–function determinants in pulmonary surfactant is needed. This review will focus on the biophysical properties of surfactant membranes, paying attention to the importance of ordered/disordered phase coexistence in such membranes.

2. The repertoire of surfactant lipids and proteins

The material isolated from cell-free bronchoalveolar fluid (BAL) consists of approximately 90 wt.% lipids (mainly phospholipids, PL) and 10 wt.% proteins. Lung surfactant is isolated from BAL by differential and density gradient centrifugation. Isolated large surfactant aggregates (LA), which consist of large membrane structures with relatively high density and very good surface activity, contain surfactant lipids and apolipoproteins SP-A, SP-B, and SP-C, but not SP-D (Fig. 2). Given that SP-D does not bind to surfactant membranes, SP-D remains in the supernatant during fractionation by ultracentrifugation. This fraction also contains small phospholipid vesicles, known as small surfactant aggregates (SA), with poor surface activity, and other proteins and peptides present in the alveolar fluid.

The lipid composition of mammalian extracellular surfactant (large aggregates) is strikingly similar to that of intracellular surfactant stored in lamellar bodies (characteristic inclusion organelles of surfactant produced by type II cells [14]) and is remarkably similar among diverse species. The lipids consist mainly of PL (~90–95 wt.%) with a small amount of neutral lipids (~5–10 wt.%), primarily cholesterol, and α-tocopherol that functions as anti-oxidant and could play a membrane structural role, comparable to that of cholesterol [4,15,16]. Among PL, phosphatidylcholine (PC) is the most prevalent class, accounting for ~80 wt.% of the total PL. Among PC molecular species, dipalmitoylphosphatidylcholine (DPPC) (16:0/16:0-PC) is the most predominant molecular species, accounting for ~55 mol% (in human [17,18], rat [19], pig, and mouse [18]) to ~40 ± 5 mol% (in goat [20], caw [19,21], and rabbit [17]) of the total PC. This saturated phospholipid can be packed to a very high density at the air–water interface, providing the large reductions of surface tensions required to stabilize the lung at the end of expiration. The remaining PC molecular species are mainly unsaturated, containing monoenoic and dienoic fatty acids sterifying the *sn*-2 position of the glycerol backbone, e.g., palmitoyl–oleoyl phosphatidylcholine (POPC) (16:0/18:1-PC). The acidic phospholipids, phosphatidylglycerol (PG) and phosphatidylinositol (PI), are mainly unsaturated and account for 8–15 wt.% of the total surfactant phospholipid pool. Other phospholipid classes are present at very low levels: unsaturated phosphatidylethanolamine (PE), sphingomyelin (SM), lyso-PC, and choline plasmalogens.

The most outstanding feature of surfactant lipid composition is not only the high proportion of DPPC, a high T_m PL, but the fact that lung surfactant consists of equimolar amounts of saturated and unsaturated phospholipid species and cholesterol. Surfactant composition suggests

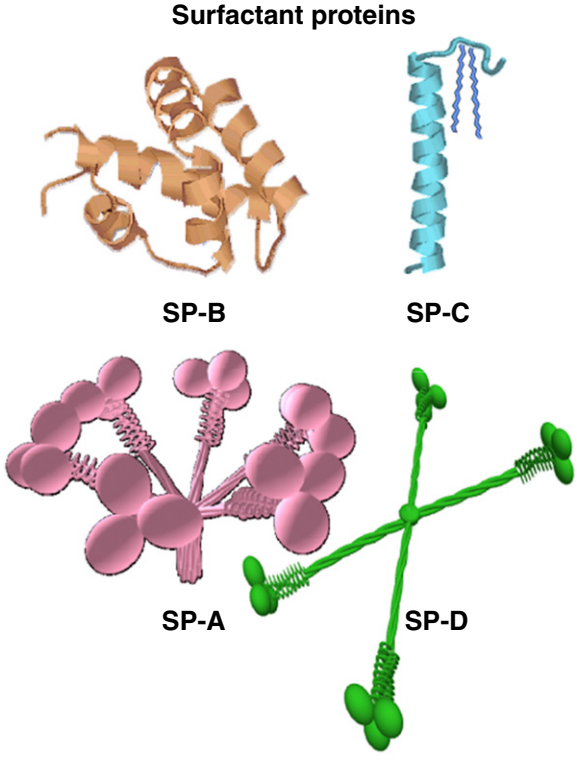

Fig. 2. Three-dimensional models of surfactant proteins. Models of the hydrophilic surfactant proteins SP-A and SP-D were constructed based on electron microscopy pictures of these proteins and the three-dimensional structure determined for trimers of SP-A [39] and SP-D [40] composed of C-globular and neck domains. The structural model of SP-C is based on the conformation of the protein determined by NMR in organic solvents [27]. The structural model of SP-B is based on predictive studies of the potential position of helical segments in the protein.

that ordered/disordered domains coexist in surfactant membranes, as has been demonstrated (see Section 4.2) thanks to the methodological development of imaging techniques that allow greater resolution.

In addition to the lipid component, there are three surfactant apolipoproteins associated with surfactant membranes. SP-B is a small hydrophobic protein that is essential for lung function and pulmonary homeostasis after birth. SP-B constitutes 0.7% of the total mass of isolated surfactant [22]. Genetic absence of SP-B in both humans and mice results in a lack of alveolar expansion and a lethal failure of pulmonary function [8,10]. In contrast, genetic absence of SP-C, another small hydrophobic protein that constitutes 0.5 wt.% [22], results in normal expansion of alveoli and pulmonary function since SP-B is sufficient for surfactant function in vivo [8,10]. However, SP-C seems to play an important role in lung innate host defense since the lack of SP-C in *SFTPC*−/− mice increases markers of macrophage alternative activation associated with diminished pathogen response and advancing pulmonary fibrosis [23,24]. In addition, mutations in genes encoding SP-C (*SFTPC*) have been linked to familial interstitial lung disease [8,25]. A recent study also reported an association between two heterozygous mutations in the *SFTPA2* gene and familial pulmonary fibrosis [26]. These results suggest that the mutations caused misfolding and trapping of human SP-A2 in the endoplasmic reticulum that could lead to loss of misfolded SP-A2 in the airspaces. It seems that, like SP-C, SP-A mutations have more severe consequences than inactivated expression of SP-A gene.

Fig. 2 illustrates three-dimensional models of SP-B and SP-C. Mature SP-C is a very small hydrophobic peptide of thirty-five amino acids. It is one of the most hydrophobic peptides known. Its structure is characterized by a hydrophobic α-helix composed essentially of valine residues and a positively charged N-terminal segment with two palmitoylated cysteines. Its three-dimensional structure has been determined by NMR in chloroform/methanol solutions [27], consisting of a very regular and rigid α-helix covering approximately two thirds of the sequence and an unstructured N-terminal segment containing prolines and the palmitoylated cysteines. In membranes, the helical segment of SP-C adopts a transmembrane orientation [28]. SP-C α-helix is stable within a lipid membrane in the fluid state but is unstable in aqueous organic solvent where it is transformed into insoluble β-sheet aggregates, which lead to amyloid fibrils [29]. With respect to SP-B, unfortunately, the three-dimensional structure of the full-length protein is not known, but high-resolution structures of synthetic protein fragments (e.g., N-terminal 1–25 [30] or 34-residue mini-B [31]) are available. Analysis of the sequence of SP-B reveals that this protein belongs to the family of the saposin-like proteins. SP-B structure might have a characteristic saposin fold with four α-helices connected by unstructured loops and linked by three intramolecular disulfide bridges [32,33]. Unlike saposin-like proteins, SP-B is a monotopical integral membrane protein. It is thought that SP-B is inserted in bilayers or monolayers with the main axis of its amphipathic helical segments aligned parallel to the plane of phospholipid layers [34,35]. Although it has been reported that both hydrophobic proteins SP-B and SP-C alter lipid packing in surfactant membranes and enhance the surface tension-lowering activity of the lipids [2,10,22], recent studies indicate that SP-B is fundamental for promoting low minimum surface tensions and stability, whereas the presence of SP-C alone may actually have negative influence on both parameters [36]. However, SP-C seems to play an important role in lung innate host defense [23,24].

Fig. 2 also shows three-dimensional models of SP-A and SP-D. These proteins are structurally characterized by an N-terminal collagen-like domain connected by a neck domain with globular C-terminal domains. The C-terminal domain includes a C-type carbohydrate recognition domain (CRD) [7,37]. These proteins are assembled in multiples of three subunits due to their collagen domain [37,38]. Supratrimeric assembly can have a cruciform type (SP-D) or bouquet type (SP-A). The three-dimensional structures of human SP-A and SP-D trimers composed of C-terminal and neck domains have been determined [39,40]. SP-A comprises approximately 3–5% of the total mass of surfactant and is mainly associated with surfactant membranes [2,41]. In contrast, SP-D constitutes about 0.5 wt.% and is not associated with lipids [2]. SP-A's ability to bind to surfactant membranes improves the adsorption and spreading of surfactant membranes onto an air–liquid interface [41], protects surfactant biophysical activity from the inhibitory action of serum proteins [4], and allows SP-A to position and concentrate together with surfactant membranes at the front lines of defense against inhaled toxins or pathogens [9,37,42].

3. Extracellular surfactant membrane polymorphism

After surfactant secretion by epithelial type II cells [43], morphological transformations take place in the alveolar fluid (Fig. 3). The secreted, tightly packed surfactant membranes rapidly transfer surface-active material to the air–liquid interface, forming the surfactant monolayer [44–46]. After de novo adsorption, the surfactant film is periodically compressed during exhalation and expanded during inhalation. Compression involves changes in surface tension (γ) from ~23 mN/m to ~1 mN/m to prevent alveolar collapse, whereas film expansion increases γ to a maximum of 20–25 mN/m to maintain alveolar stability.

Several lines of evidence indicate that mechanical properties of surfactant films do not depend only on the behavior of a single monolayer. Studies using electron microscopy [47,48], atomic force microscopy (AFM) [49,50], neutron reflection [51], and captive bubble tensiometry [48,52] indicate that the interfacial film is thicker than a single monolayer. Thus the surface film consists of a surface monolayer plus one or more lipid bilayers, closely and apparently functionally associated with the interfacial monolayer. The cohesivity of these layers also contributes to sustain the low γ reached at the end of exhalation. Fig. 3 illustrates pulmonary surfactant absorption to the interface from secreted lamellar body-like particles and the surfactant film attached to a continuous network of surfactant bilayers. Multilayer formation could arise from the multilaminations of lamellar bodies.

Surfactant adsorption, which means bilayer to monolayer transformation, occurs in a surface tension-dependent manner. It is activated above the equilibrium surface tension (γ_e) (~23 mN/m) and decreases when γ falls below γ_e [44,45]. Using molecular dynamics simulations, Baoukina and Tieleman [53] show how SP-B, in a characteristic saposin-fold structure that may interconvert between extended and bent conformations, might mediate the formation of a stalk-like structure between bilayer aggregates in water and the interfacial monolayer. A lipid flow might occur between the monolayer and the vesicle via the stalk. The direction of the flow would depend on the γ in the monolayer. Below γ_e (~23 mN/m), lipids are transferred from the monolayer to the vesicle. Above the equilibrium tension, lipids are transferred from the bilayer to the monolayer. Thus SP-B might facilitate lipid transfer between these structures in a surface tension-dependent manner. These molecular dynamics simulation studies are consistent with the reports by Chavarha et al. [54] and Farver et al. [55] that lipid polymorphism induced by surfactant hydrophobic proteins is required to promote adsorption.

Fig. 3 also shows highly organized structures termed “tubular myelin” that are formed when SP-A reacts with secreted lamellar bodies Tubular myelin is composed of large square elongated tubes comprised primarily of phospholipids and proteins. In vitro reconstitution of tubular myelin requires the presence of DPPC, PG, SP-A, SP-B, and Ca^{2+} [56]. Animals with inactivated expression of SP-A lack TM [57] and do not show any apparent respiratory dysfunction upon birth, suggesting that TM does not have an essential role in the biophysical function of pulmonary surfactant. The mechanism involved in the formation of tubular myelin is poorly understood, as is the functional significance of these complex structures. Morphological studies

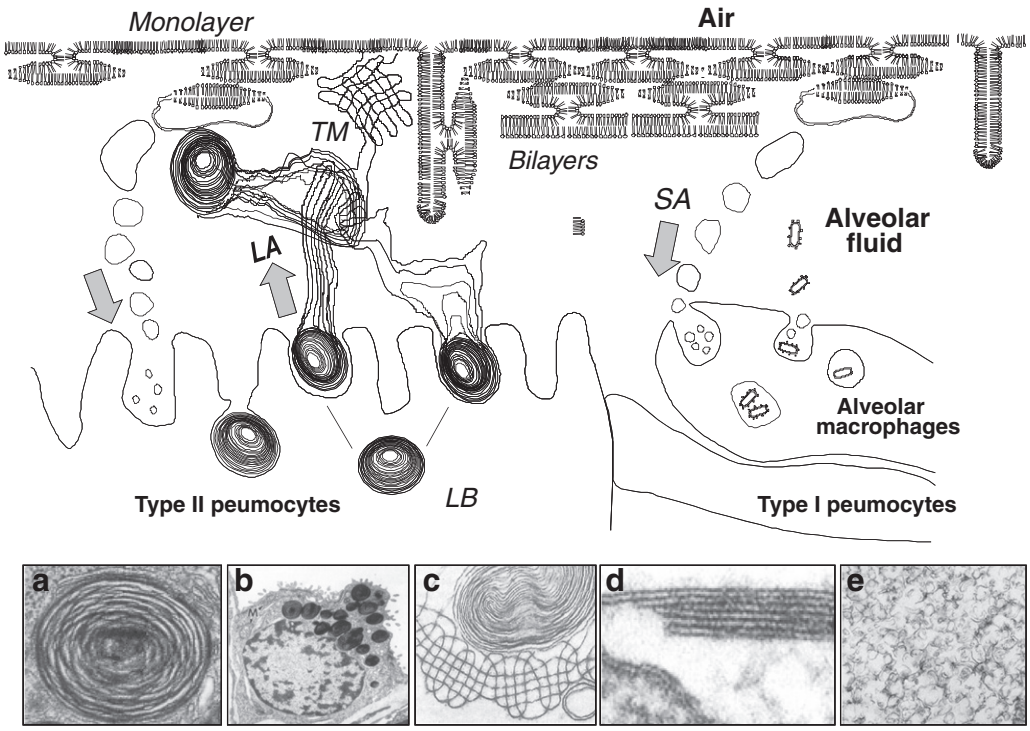

Fig. 3. Extracellular surfactant membrane polymorphism. The pulmonary surfactant is synthesized by type II epithelial cells and stored as tightly packed bilayer membranes in characteristic intracellular inclusions called lamellar bodies (LB) (a). After regulated secretion by exocytosis (b), LB unravel spontaneously in the alveolar fluid to form multilamellar vesicles and highly organized membranes termed tubular myelin (TM) (c). These large extracellular membranes, called large surfactant aggregates (LA), have high surface activity. They adsorb very rapidly to the air–liquid interface. The surface film at the alveolar air/liquid interface consists of a phospholipid monolayer with bilayer structures attached to it (d). With surface compression and expansion cycles, small vesicles are generated (E). These vesicles are named small surfactant aggregates (SA) and have poor surface activity. Small aggregates are taken up and degraded by alveolar macrophages and type II cells. Images shown in this figure have been reproduced with permission from (a–c) [14], (d) [47], and (e) [58].

indicate that tubular myelin figures are in close proximity to the surface layer of the alveolar fluid [14]. McCormack and Whitsett [42] suggested that tubular myelin could have a primary antimicrobial function that would serve to collect inhaled microbes at the air–liquid interface due to the high concentration of SP-A in these structures. It seems possible that surfactant membranes and their apolipoproteins simultaneously function as the primary antimicrobial defense in the alveolar fluid and as a protective layer against alveolar collapse.

With repetitive surface compression and expansion cycles, small vesicles may be generated (SA) [58] (Fig. 3). The used and rejected surfactant material, with poor surface activity, is taken up continuously by alveolar macrophages and epithelial cells in the form of small lipid vesicles. Type II cells recycle part of surfactant's components into lamellar bodies. Thus alveolar cells are always in contact with surfactant membranes and ingest abundant amounts of this material. The effects of these surfactant vesicles on macrophage activation state and on epithelial cells remain unclear. The loss of surfactant from the airspaces is balanced by secretion of surfactant stored in lamellar bodies. The estimated turnover period of lung surfactant ranges from 4 to 11 h [59]. However, the modulation of pathways involved in the balance between the intracellular storage pool and the extracellular functional pool is unknown.

4. Phase behavior of surfactant membranes in the alveolar spaces

Surfactant membranes play a crucial role in surfactant biophysical function. The mechanical properties of the interfacial film, and hence the response of surfactant membranes to the breathing cycle, are determined by their physical state. Discussion of the role of surfactant membranes on the biophysical properties of pulmonary surfactant requires some knowledge about lipid phase transitions and lateral phase segregation. Therefore, we briefly review the phase behavior of surfactant membranes (bilayers and monolayers) in comparison with DPPC membranes, since this saturated phospholipid is the main phospholipid component in lung surfactant and has traditionally been thought responsible for lowering surface tension to near-zero values at physiological temperatures.

4.1. Phase transitions in surfactant bilayers and the surface-active film in comparison with DPPC bilayers and monolayers

When DPPC molecules are dispersed in an aqueous phase, they arrange themselves into a closed bilayer, where the hydrophobic fatty acid groups point toward the center of the bilayer in order to minimize the unfavorable interactions between the bulk aqueous phase and the hydrocarbon fatty acid chains. A characteristic property of lipid membranes is their ability to undergo phase transitions induced by temperature [60]. The DPPC bilayer can exist in either a liquid-crystalline (L_α) or a gel ($L_{\beta'}$) phase. The temperature at which this transition takes place is known as the transition or melting temperature (T_m) [60,61]. Bilayers composed of DPPC exhibit two phase transitions induced by temperature, a pretransition from the gel ($L_{\beta'}$) to the ripple phase ($P_{\beta'}$) [62], and a very sharp $P_{\beta'}/L_\alpha$ transition with a melting temperature of 41 °C (Fig. 4A). Thus DPPC bilayers in the $L_{\beta'}$ phase can melt to a L_α phase by increasing temperature.

These two phases ($L_{\beta'}$ and L_α) are defined by the strength of the attractive Van der Waals interactions between adjacent lipid molecules [63]. The tight packing of the DPPC molecules in the gel phase, which is due to the all-trans configuration adopted by the fatty acid acyl chains, gives rise to strong interactions between the hydrophobic tails of the lipid molecules [63]. Consequently, lipids in $L_{\beta'}$ state are highly ordered and remain relatively immobile, exhibiting neither lateral nor rotational mobility. In the liquid-crystalline phase, L_α, individual DPPC molecules can have rotational and translational motions

within each leaflet of the bilayer, which confers fluidity to the bilayer [64]. For this reason, the liquid-crystalline phase is also known as the fluid phase. Moreover, in L_α phase, phospholipid fatty acid chains undergo trans-gauche isomerization at their C–C bonds [65], which tends to expand the area occupied by the chains, reducing the lipid packing and hence the strength of the interactions between adjacent molecules. Trans-gauche isomerizations confer relative disorder to the phospholipid acyl chains [63,65]; for this reason, the L_α fluid phase is also usually referred to as the liquid-crystalline disordered phase (L_d).

This phase behavior is altered by the presence of cholesterol. The general trend is that cholesterol has a fluidizing effect on lipids in the gel phase (below T_m) because the intercalation of the planar steroid molecules reduces lipid packing [66]. At the same time, cholesterol has a condensing effect on phospholipids in the fluid phase (above T_m) because cholesterol promotes an acyl chain extension due to restriction in the chain's ability to undergo *trans-gauche* isomerization [67,68]. The presence of cholesterol generates a new phase referred to as liquid-ordered phase (L_o) in which the orientational order of the acyl chains is similar to that characteristic of the gel phase ($L_{\beta'}$), but phospholipids in L_o phase exhibit lateral diffusion rates and rotational motions slightly smaller but of the same order of magnitude as in L_d [67,68]. Thus L_o has properties intermediate between the gel ($L_{\beta'}$) and fluid-disordered state (L_d). L_o is an ordered phase from the point of view of the conformational structure of the lipid chains but a fluid phase from the point of view of lateral and rotational mobility of the molecules [67,69]. Thus the fluidity of the bilayers would be $L_{\beta'} < L_o < L_d$, whereas the lipid order would be $L_{\beta'} > L_o > L_d$.

Cholesterol is more soluble in the fluid phase and preferentially partitions into this phase, although, at the same time, it has a preference for ordered acyl lipid chains [69]. The actual phase behavior of DPPC/cholesterol mixtures depends greatly on both the temperature and the cholesterol mol fraction. For cholesterol concentrations between 10 and 23 mol%, which correspond to the amount of cholesterol determined in both alveolar and lamellar body surfactant [70], cholesterol broadens and reduces the enthalpy and temperature of the main transition [71]. Phase diagrams indicate that for cholesterol concentrations between 10 and 23 mol%, lateral phase separation occurs and there is L_o/L_d phase coexistence at temperatures above T_m and $L_o/L_{\beta'}$ phase coexistence at temperatures below T_m [72]. However, for cholesterol concentrations above 30 mol%, only L_o prevails over a wide temperature range [72] and the main transition of DPPC is

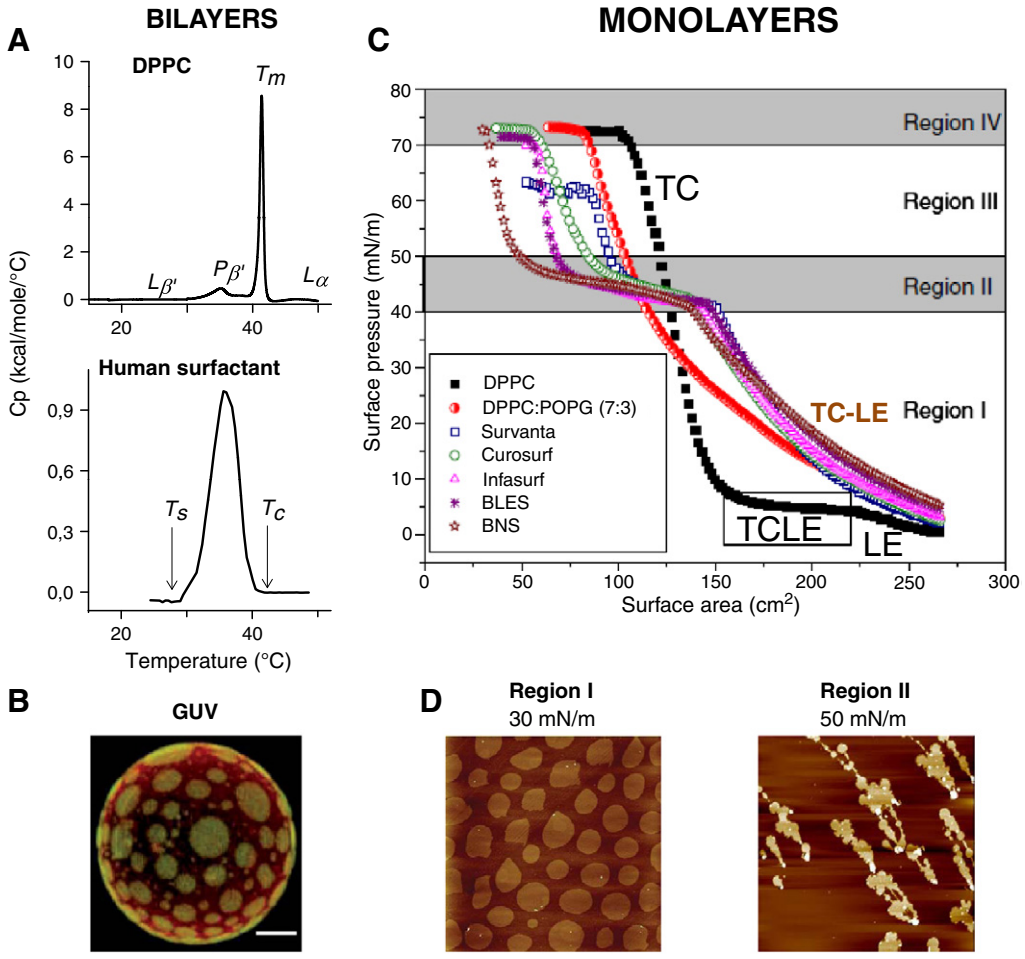

Fig. 4. Lipid phase transitions and lateral phase separation in surfactant bilayers and monolayers. A: Differential scanning calorimetry thermograms of DPPC and native surfactant from healthy subjects. DPPC exhibits two transitions: a pretransition from the gel ($L_{\beta'}$) to the ripple ($P_{\beta'}$) phase, and the main transition from $P_{\beta'}$ to the liquid-crystalline (L_α) phase. Human surfactant shows a broader transition with lower enthalpy. T_m, the transition midpoint temperature; *Ts*, the onset or lower boundary of the phase transition; *Tc*, the completion or upper boundary temperature. Adapted from [74]. B: GUVs of native porcine surfactant are doped with the fluorescent probe DiIC18 (red [L_o]) and Bodipy-PC (green [L_d]) and exhibit liquid-ordered/liquid-disordered (L_o/L_d) phase coexistence at 37 °C. C: Phase behavior of various clinical and natural surfactant monolayers in comparison with pure DPPC films at 20 ± 1 °C. Four pressure-dependent regions are detected for the compression isotherms of clinical and natural surfactants: Region I. Monolayer region at $\pi \leq 40$ mN/m; Region II. Monolayer-to-multilayer transition region at $40 < \pi < 50$ mN/m; Region III. Multilayer region at $\pi \geq 50$ mN/m; and Region IV. Collapse region. Graph taken from [79] with permission. D: AFM images of native rat surfactant monolayers at 24 ± 1 °C. At 30 mN/m, TC circular micro-domains are observed within the LE phase. At 50 mN/m, monolayer-to-multilayer transition occurs and stacks of bilayers appear.
AFM pictures have been reproduced from [19] with permission.

obliterated. Micron-scale coexisting liquid phases were initially reported in giant unilamellar vesicles (GUVs). Ternary mixtures of a high T_m lipid (DPPC), a low T_m lipid (Dioleoyl-PC, but not POPC), and cholesterol (a mixture similar to surfactant membrane lipids) form large coexisting liquid domains (L_o and L_d) over a wide range of compositions and temperatures [73].

Fig. 4A also shows that, compared to DPPC, the thermal transition of bilayers from human lung surfactant exhibits a broader melting event with lower melting enthalpy (ΔH) due to the complex lipid composition of these membranes and the presence of cholesterol [74]. Surfactant bilayers of healthy humans exhibit a T_m of 37.2 ± 0.1 °C in the presence of calcium, which shifts slightly downward (36.2 ± 0.1 °C) in its absence [74], and a completion temperature (T_C) of ~41 °C. Over a wide temperature range (from 25 °C to the completion temperature) surfactant membranes show micron-scale coexisting liquid phases as described in the Section 4.2. Fig. 4B shows a giant unilamellar vesicle formed from surfactant membranes labeled with DiIC18 (red) and Bodipy-PC (green). The rounded green areas in the image correspond to fluid-disordered phase, enriched in unsaturated phospholipids. The red background corresponds to ordered phase, enriched in high T_m phospholipids (such as DPPC and SM).

As stated above, pulmonary surfactant membranes arrange as a monolayer at the air/water interface, with the lipid polar headgroups oriented toward the aqueous phase, whereas the fatty acid chains extend into the air, avoiding contact with water. Lipid packing, and hence the different phases in which lipids can exist in an interfacial monolayer, is defined at a given temperature by changes in compression. Thus it is possible to increase the Van der Waals interactions between lipid molecules by reducing the surface area available per lipid molecule, giving rise to different lipid phases. Compression of surfactant monolayers can be achieved *in vivo* during breathing cycles or *in vitro*, in a surface balance, either by depositing additional lipid molecules in the interface, which will increase the surface concentration, or by moving a barrier across the surface [4,5,75]. As the amount of lipid molecules in the interface increases, the surface tension at the air–water interface decreases, leading to a detectable increase in surface pressure. Surface pressure, π, is defined as

$$\pi = \gamma_0 - \gamma$$

where γ_0 is the surface tension of the clean air–water interface and γ that of the surface covered by the lipid monolayer. The dependence of surface pressure on the surface area available per lipid molecule constitutes the compression isotherm.

Fig. 4C shows the surface pressure–area (π–A) isotherms obtained at 25 °C for monolayers of DPPC. At low compression levels, the monolayer is in the liquid expanded (LE) phase. This phase is characterized by low lipid packing and considerable configurational freedom at the interface due to the presence of trans-gauche isomerizations [75]. Further compression of the monolayer gives rise to a transition from LE to a highly packed state known as tilted condensed (TC) phase where all of the acyl groups are in the extended all-trans configuration [75]. At a given temperature, the range of surface pressures at which the LE/TC transition takes place depends on the nature of the aqueous subphase. The LE/TC transition, reflected in the compression isotherm as a plateau, takes place in the range of 7–12 mN/m on a buffered saline subphase containing physiological amounts of NaCl or in the range of 3–5 mN/m on a pure water subphase [76,77]. Compression of the monolayer to the TC phase can only be achieved at temperatures below the corresponding T_m of bilayers of the same composition. Due to the high T_m of DPPC, the acyl chains of DPPC can be packed to a very high density at the air–water interface at physiological temperatures, providing the large reduction of surface tensions necessary to prevent alveolar collapse at end expiration [75]. A further reduction in surface area leads to film collapse, with irreversible loss of monolayer components. As described above for lipid bilayers, incorporation of cholesterol into the interfacial film might alter the phase behavior of the lipids. It has recently been reported that DPPC–cholesterol monolayers display a phase of intermediate order between TC and LE phases [78], which might be referred to as LO phase [19,79]. Cholesterol shows a preference for the interface between TC and LE phases [78]

Compared to DPPC films, the surface pressure–area (π–A) isotherms from monolayers of native lung surfactant or replacement surfactants show a plateau region at π of 40–50 mN/m (Fig. 4C). Zhang et al. [79] have identified four π-dependent regions for natural and modified surfactants, based on film structures revealed by AFM. Region I corresponds to π in the range of 10 to 40 mN/m. Over this wide range of π, phase coexistence between ordered and disordered regions in the monolayers occurs, as can be observed from AFM images [79] (Fig. 4D). In rat lung surfactant the area covered by ordered micro-domains increases with increasing surface pressure [19]. The second region, in the surface pressure interval from 40 to 50 mN/m, refers to the monolayer-to-multilayer transition at the equilibrium spreading pressure, π_e. The third region covers a π range from ~50 to 72 mN/m, which represents the physiologically relevant π range. In this region, the interfacial monolayer is attached to squeezed out bilayers. It is thought that this 3D structure composed of bilayers functionally attached to the interfacial monolayer contributes to sustain the low γ reached at the end of exhalation [53,80,81]. The fourth region refers to the collapse of surfactant films. The collapse pressure (π_c) is the maximum π that can be reached and sustained by a phospholipid film under lateral compression. Surfactant films without cholesterol appear to collapse at π_c with a folding mechanism, whereas surfactant films with cholesterol appear to collapse with a protrusion mechanism, in which multilayered protrusions are uniformly nucleated throughout the entire film [79].

4.2. Lateral phase separation in surfactant bilayers and monolayers

The special composition of surfactant membranes, which consist of equimolar amounts of saturated and unsaturated phospholipid species and cholesterol, suggested the presence of ordered/disordered phase coexistence under physiological conditions, based on the information obtained in POPC/DPPC/Cholesterol model systems [73]. In the last decade, the lateral structure of bilayers has been explored using techniques that provide spatial resolutions that range from nano- (AFM) to micrometers (fluorescence microscopy, FM). FM and related techniques (such as fluorescence lifetime imaging, fluorescence correlation spectroscopy, anisotropy imaging) provide a lateral resolution limit of ~300 nm and require the use of fluorescent probes. AFM detects height differences among various regions of supported membranes (monolayers and/or bilayers) and does not require the use of probes. To determine lateral phase segregation in surfactant membranes, both microscopy techniques have been used.

Bernardino de la Serna et al. [82] demonstrated that GUVs composed of native lung surfactant membranes display micrometer-sized ordered/disordered phase coexistence at physiological temperatures (Fig. 4B). Phase coexistence depends on the lipid component because the absence of SP-A or the extraction of the hydrophobic proteins SP-B and SP-C from surfactant membranes does not change the characteristic phase coexistence of surfactant membranes. In native porcine surfactant phase coexistence occurs from 22 to 40 °C. Most of the micro-domains were abolished at 40 °C [82,83]. Given that the melting process of human lung surfactant terminates above 41 °C (Fig. 4A), phase coexistence may occur at physiological temperatures (36–37 °C) and decrease in feverish states.

Based on the particular round shape of the domains and the partition properties of the different fluorescent probes used to label surfactant membranes, the lateral organization of porcine surfactant vesicles was ascribed to fluid ordered/fluid-disordered-like phase coexistence [82–84]. The nature of ordered domains was also

assessed by cholesterol extraction from the native material using methyl-β-cyclodextrin. However, given that fluorescence microscopy distinguishes L_o and L_α phases, but not $L_{\beta'}$ and L_o phases, it is possible that coexisting $L_{\beta'}$, L_α, and L_o phases were present in surfactant membranes over a range of temperatures. However, lateral diffusion coefficients, determined in NMR experiments [83], indicate that the two types of domains segregated in surfactant bilayers have a dynamic character, suggesting a fluid–fluid (L_o/L_α) phase coexistence. Unlike the interfacial surfactant monolayer that should be quite rigid, surfactant membranes present in the alveolar fluid seem to be dynamic. Synthetic surfactants, which consist of combinations of synthetic lipids and either synthetic or recombinant peptides, and some animal-derived replacement surfactants show gel/fluid phase coexistence, instead of fluid–fluid phase coexistence, as a consequence of the lipid composition and/or the lack [74,85] or reduced content of cholesterol [86].

Lateral phase segregation has also been observed in interfacial films formed by adsorption of lamellar body-like particles secreted by rat alveolar type II cells [46]. Using an inverted fluorescence microscope, Ravasio and co-workers demonstrated that the film formed by the adsorbed material spontaneously segregates into distinct liquid-ordered (LO), liquid-disordered (LE), and gel-like (TC) regions under near-physiological conditions (at 37 °C and 100% rH). The most remarkable property of monolayers formed from lamellar body-like particles is their solid-like character. The authors propose that condensation and solidification of the interfacial monolayer, even in the absence of external lateral compression, could occur through an active ejection of material into the interface. In fact, progressive adsorption of lamellar body-like particles led to the appearance of large, protruding three-dimensional structures, presumably accumulating multilayered material projected toward the subphase. Using different approaches, Keating and co-workers [81] recently showed that multilayers start to form at the edge of the solid-like (TC) domains and also in the fluid-like (LE) phase. Moreover, time-of-flight secondary ion mass spectrometry (ToF-SIMS) analysis indicated that multilayer structures are enriched in unsaturated PLs while the saturated PLs are concentrated in the remaining interfacial monolayer, which supports the solid-like character of the interfacial monolayer at physiological surface pressures (~45–72 mN/m).

Different lipid phases have also been observed in native surfactant monolayers using different techniques: AFM [19,20,79–82,87–89], ToF-SIMS [81,89,90], epifluorescence microscopy [86,91–93], and Brewster angle microscopy [93]. There is evidence that circularly-shaped TC micro-domains appear at low surface pressure and increase in area coverage with increasing π up to a surface pressure of around 35–45 mN/m. Interestingly, goat surfactant films exhibit elongated noodle-shaped domains, instead of circular domains, that increase in size and length up to 40 mN/m [20]. The elongated morphology of the domains was attributed to the low cholesterol content (0.6% by weight) in this surfactant, which would decrease the line tension. In addition to TC micro-domains, TC nano-domains were observed by AFM within the LE phase. In rat surfactant, the area covered by the nano-domains decreased with increasing π to less than 1% of the surface area [19]. However, bovine surfactant monolayers exhibit a decrease in micro-domains with a corresponding increase in nano-domains with increasing π [19,79]. A significantly higher proportion of disaturated PC was found in rat surfactant (~60 mol% of total PC species) compared with bovine surfactant (~40 mol%) [19]. Several factors might contribute to the micro- and nano-domain formation within the surfactant monolayer: the specific phospholipid profile (relative percentage of saturated and unsaturated phospholipids), hydrophobic protein content, cholesterol content, and surface pressure [19,79]. On the other hand, coexistence of different lipid phases has also been determined in monolayers from purified surfactant phospholipids, without hydrophobic proteins [94–96] and in lipid mixtures containing SP-C [97,98] and SP-B [90,99].

With respect to lipid and integral membrane protein (SP-B and SP-C) partitioning in ordered and disordered domains of surfactant monolayers, combined ToF-SIMS and AFM studies [81,89] show that saturated and unsaturated phospholipids segregate into different domains in both bovine and rat surfactant monolayers. With respect to hydrophobic surfactant proteins, it has been shown that SP-B and SP-C distribute preferentially in fluid regions of interfacial films [89]. Segregation of hydrophobic proteins in the fluid phase has also been determined in surfactant-like lipid mixtures [100–104]. SP-B and SP-C also segregate into fluid regions of surfactant bilayers because the fluorescence of these proteins colocalized with the Bodipy-PC-fluid areas when fluorescently labeled SP-B and SP-C were incorporated into giant unilamellar vesicles composed of surfactant lipids [82]. With respect to SP-A, epifluorescence microscopy studies show that SP-A interacts with the ordered or gel-like regions of native surfactant monolayers and/or attached bilayers [92] and with TC regions of surfactant-like lipid monolayers [105,106]. SP-A causes a reorganization or rearrangement of solid domains in the surfactant monolayer, which is consistent with its activity to promote membrane–membrane aggregation [37,38,41,107,108].

5. Significance of ordered/disordered phase coexistence in surfactant biophysical function

It is generally accepted that adsorbed surfactant material forms a stable monolayer at the air–liquid interface capable of tolerating high lateral compression during expiration, which implies that the monolayer becomes enriched in solid-like phase and quite rigid. In addition, the monolayer should be able to re-expand during inspiration (Fig. 5). The role of lateral phase segregation in lung surfactant function is unclear, but lipid lateral organization might be important to sustain a solid-like film attached to a continuous network of highly dynamic membranes.

Surfactant membranes connected to the surfactant monolayer are thought to be essential for lung surfactant function [4–6,47–52,97,103,104,109–111]. A potential mechanism for attaining high π (low γ) during expiration can be found in the monolayer-to-multilayer transition that represents a reversible, partial monolayer collapse occurring near π_e (i.e., 40–45 mN/m). The resultant bilayer structures apparently remain closely attached to the interfacial monolayer, as they can readily respread to the monolayer during film expansion [4–6,109,110] (Fig. 5). Molecular dynamic simulations suggest that the bilayer folds remain connected to the lung surfactant monolayer and that the contact area of the lipid chains with air is reduced by approximately twice the area of the fold [112]. On the other hand, bilayer reservoirs underlying the monolayer, which could also arise from the multilaminations of lamellar bodies, are believed to play an additional role in stabilizing the interface against collapse at low surface tensions, especially if bilayers are bridged through SP-B and SP-C (Fig. 6) [4–6,110]. An important remaining question is how surfactant films with mixed disordered and ordered domains become enriched in solid-like phase to attain γ near zero during film compression.

By combining ToF-SIMS and AFM studies of bovine surfactant films at high π, Keating and co-workers have recently shown that compression-driven multilayer structures are enriched in unsaturated PLs while the saturated PLs are concentrated in the remaining interfacial monolayer [81]. Moreover, they show that multilayers start to form at the edge of solid-like TC domains and also in the fluid-like LE phase. Fig. 5 shows how phase coexistence might facilitate film folding to form three-dimensional structures enriched in fluid phase, which would promote the solidification of the interfacial monolayer during exhalation. Hence, lipid lateral organization would aid the film to attain minimal surface tension [80,81].

SP-B and SP-C, which partition preferentially in fluid regions of interfacial films [89,100–104], seem to facilitate the folding of the surfactant monolayer induced by compression, resulting in the segregation of unsaturated phospholipids from the interface. Both SP-B [53,103,104,113] and SP-C [49,102,111,114–116] promote two- to three-dimensional

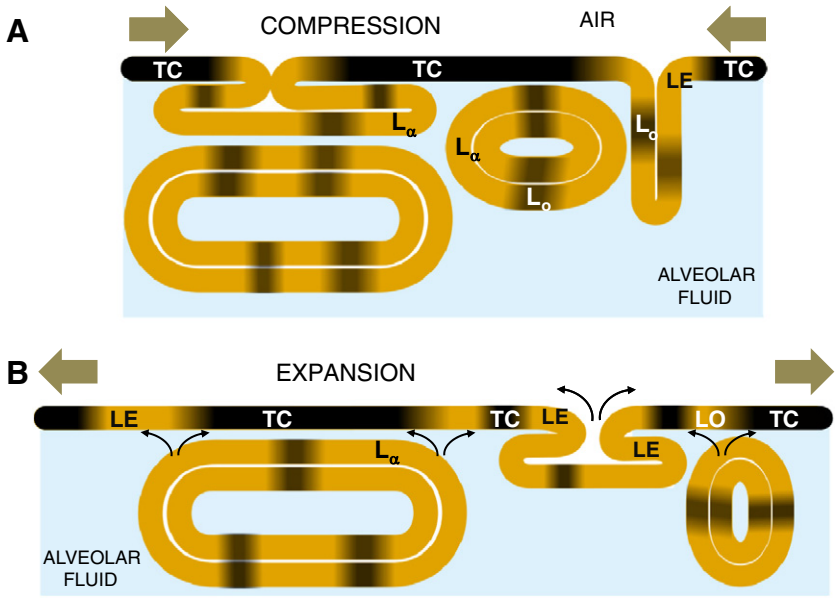

Fig. 5. Dynamic behavior of lung surfactant during respiratory compression-expansion cycling. A) Film compression (exhalation) covers a π range from ~45 to 70 mN/m (γ~23 to 0 mN/m), which represents the physiologically relevant π range. The ability of surfactant to reach very low tensions during exhalation can depend on formation of folded structures, which start to form at the edge of solid-like TC domains and also in the fluid-like LE phase [81]. The resultant bilayer structures apparently remain closely attached to the interfacial monolayer, as they can readily re-spread to the monolayer during film expansion (B). Folded structures selectively segregate fluid monolayer components [81]. Consequently, after formation of these protrusions, the interfacial monolayer would be enriched in solid-like domains so that it can reach very low surface tensions. (B) During expansion (inhalation) surface tension rises to γ_e (~23 mN/m) by re-spreading of phospholipids into the interface. Folded structures may act as a membrane reserve and attenuate the increase in membrane tension during inspiration.

transformation in monolayers. Molecular dynamic simulation studies indicate that SP-B aggregates (at least dimers) may not only form nucleation sites but bend the monolayer locally and line the highly curved perimeter of the folds [53]. SP-B has no effect on monolayers forming a solid-like TC phase. Phase coexistence is required for SP-B-induced monolayer folding [53].

SP-B and SP-C also promote exchange of phospholipids between membranes [117,118] and between membranes and interfacial monolayers [53,119,120]. This suggests that attachment of disconnected bilayers by surfactant proteins constitutes the first step in formation of a lipid-lined connection between the interface and the multilayer network in the subphase. Fig. 6 shows how SP-B and SP-C promote the establishment of membrane–membrane contacts that increase the cohesivity between surfactant layers. Moreover, the capability of SP-A to bind simultaneously to different bilayers might increase the cohesivity between surfactant membranes [5,37]. It is thought that the cohesivity of

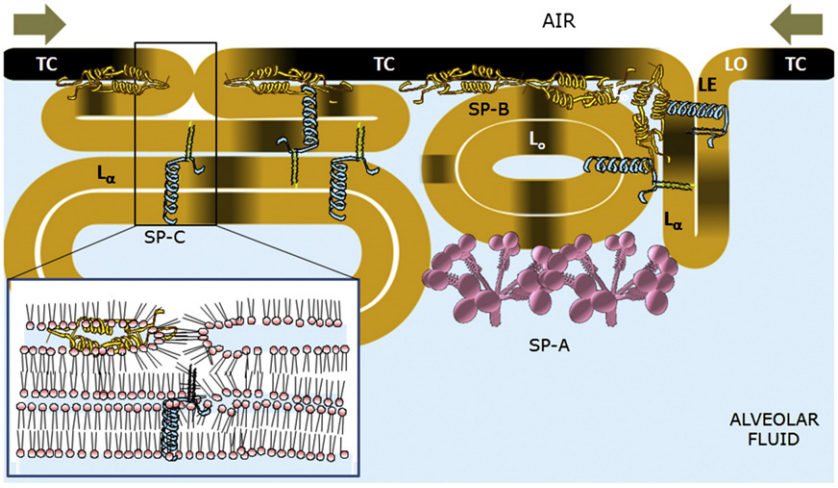

Fig. 6. Role of surfactant proteins in surfactant dynamics. Surfactant proteins facilitate the optimal dynamic behavior of surfactant during breathing. SP-B and SP-C, which partition preferentially in fluid regions of interfacial films, seem to facilitate the folding of the surfactant monolayer induced by compression [53,104,111,116], resulting in the segregation of unsaturated phospholipids from the interface [81]. SP-B has no effect on monolayers forming a solid-like TC phase. Phase coexistence is required for SP-B-induced monolayer folding [53]. In addition, attachment of disconnected bilayers by surfactant proteins constitutes the first step in formation of a lipid-lined connection between the interface and the multilayer network in the subphase. The inset shows how SP-B and SP-C promote the establishment of membrane–membrane contacts that increase the cohesivity between surfactant layers. The palmitoylated cysteines and N-terminal segment of SP-C can insert into membranes or films other than that where the hydrophobic α-helix is inserted, whereas SP-B, by adopting a bent conformation, binds to the surfaces of both membranes. Finally, the capability of SP-A to bind simultaneously to different bilayers might increase the cohesivity between surfactant membranes, which helps to sustain low γ at the end of exhalation [5].

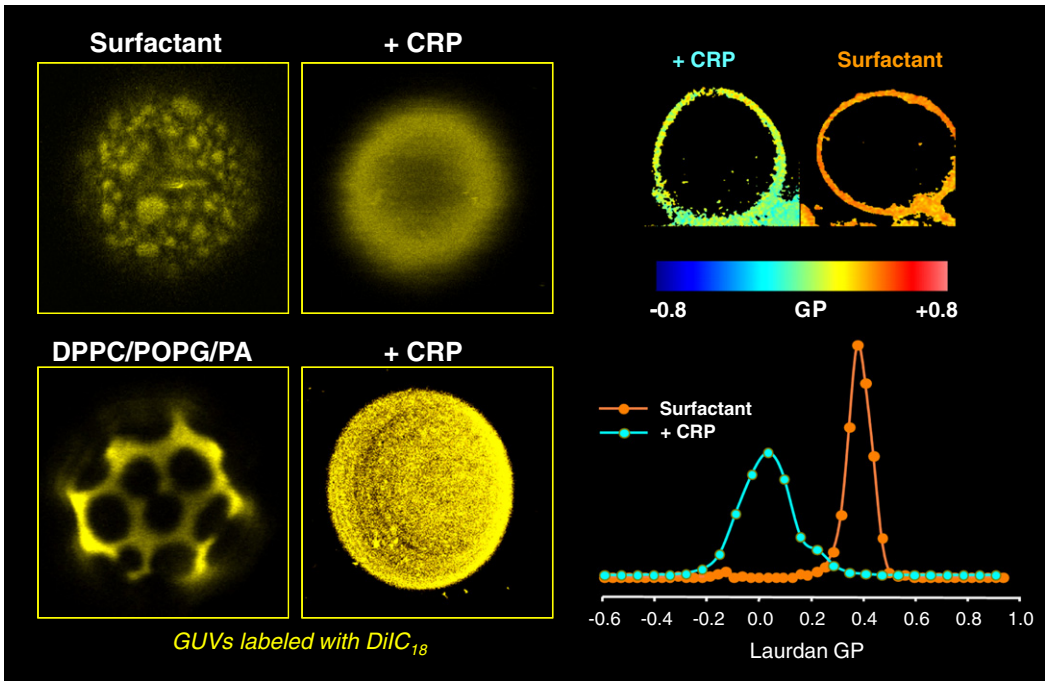

Fig. 7. CRP abolishes ordered/disordered phase coexistence and increases fluidity of surfactant membranes. *Left*, CRP effects on the lipid lateral organization of GUVs prepared from either porcine lung surfactant or DPPC/POPG/PA (28:9.4:5.1, w/w) doped with the fluorescent probe DiIC18. GUVs composed of surfactant exhibit fluorescent round domains over a dark background characteristic of liquid-ordered/liquid-disordered (L_o/L_d) phase coexistence, whereas GUVs composed of surfactant-like lipids, which contain no surfactant proteins or cholesterol, show solid/fluid ($L_{\beta'}/L_\alpha$) phase coexistence. The fluorescent dye is present in the fluid domains and excluded from the micrometer-sized solid domains, which appear black. The addition of CRP to GUVs composed of lung surfactant or surfactant-like lipids caused disappearance of the L_o/L_d phase coexistence (surfactant) or $L_{\beta'}/L_\alpha$ phase coexistence (DPPC/POPG/PA) typical of these membranes. *Right*, top row: two-photon Laurdan GP images of a single surfactant GUV in the absence and presence of 10 wt.% CRP. Bottom row: Laurdan GP histograms corresponding to the two images presented on top. At 25 °C, the Laurdan GP histogram of surfactant is centred at GP values of ~0.42. After CRP addition, the Laurdan GP value decreases to ~0.14, indicating that CRP fluidizes surfactant membranes.
Adapted from [84].

this multilayer network also contributes to sustain low γ at the end of exhalation [4–6].

6. Effect of surfactant inhibitors on ordered/disordered phase coexistence

Surfactant biophysical activity can be inactivated by incorporation of materials inhaled from the upper airways, leaked from capillaries, or secreted by alveolar cells. Surfactant inhibitors interfere with surfactant adsorption to the air–liquid interface and prevent surfactant from reaching low surface tension upon compression and re-spreading during expansion [4]. In general it is thought that only some lipids are capable of inhibiting surfactant function by mixing with surfactant components and hence altering surfactant structure. These types of inhibitors are lipids that do not form lamellar liquid–crystalline structures but can be incorporated to some degree in bilayers. These lipids are soluble amphiphilis that form micelles (such as lysophospholipids or bile acids) or insoluble non-swelling amphiphilis (such as cholesterol, diacylglycerols, or triacylglycerols). However, recent studies have demonstrated that this mechanism of surfactant inhibition involves some proteins and particles other than lipids. Here we briefly review the effects of several surfactant inhibitors that interact with surfactant membranes on both surfactant function and lateral phase separation.

C-reactive protein (CRP) is one of the proteins that have recently been found to bind to surfactant membranes [84]. CRP inserts into surfactant membranes rather than binding to the membrane surface and affects membrane physical properties. The effect of CRP on surfactant inactivation is of great interest in lung pathophysiology since CRP displays a rapid and pronounced increase of concentration in response to inflammation or infection and invades the alveolar space as a result of increased capillary permeability [121–123]. Fig. 7 shows that insertion of CRP into surfactant membranes or surfactant-like membranes composed of DPPC/POPG/palmitic acid (PA) causes disappearance of micrometer-sized ordered/disordered phase coexistence. In the presence of CRP, DiI_{C18} fluorescence is uniform over the GUV surface, suggesting that ordered domains are much smaller than the optical resolution of the microscope [84]. Consistent with this morphological information, Laurdan fluorescence experiments demonstrated that CRP drastically affects membrane fluidity. Laurdan generalized polarization images of single GUVs using two-photon excitation fluorescence microscopy indicate that CRP decreases the Laurdan GP value from 0.4 to 0.1, indicating that CRP has a strong fluidizing effect on these membranes [84]. These alterations in membrane fluidity and lipid lateral organization correlate with the fact that intratracheal instillation of CRP in rat lungs causes surfactant inactivation [84]. In addition, CRP hinders lung surfactant function *in vitro:* surfactant is unable to reach very low surface tensions during dynamic film compression and to adsorb to an air–water interface in the presence of CRP [122–126]. Altogether, these data indicate that CRP-induced alterations in membrane fluidity and lipid lateral organization correlate with CRP-induced lung surfactant inactivation as demonstrated by *in vitro* and *in vivo* studies.

Serum albumin, which also invades the alveolar space in acute lung injury, has also been shown to affect the structure and function of surfactant material. Incorporation of albumin molecules into bovine lung surfactant monolayers interferes with their dynamic surface activity [88,127] and disturbs the characteristic phase coexistence in bovine lung surfactant films, preventing the formation of TC domains [88]. Albumin also alters the formation of multilayered structures, which show smaller sizes and single-bilayer thicknesses [88].

Surfactant function is also impaired by cholesterol. While endogenous levels of cholesterol (about 14–20 mol% or 8–10 wt.% in most mammals [70]) have no negative effects on surfactant function, supraphysiological amounts of this sterol have a deleterious effect [4]. Fig. 8 shows how elevated levels of cholesterol (20 wt.%) reduce the ability of surfactant to

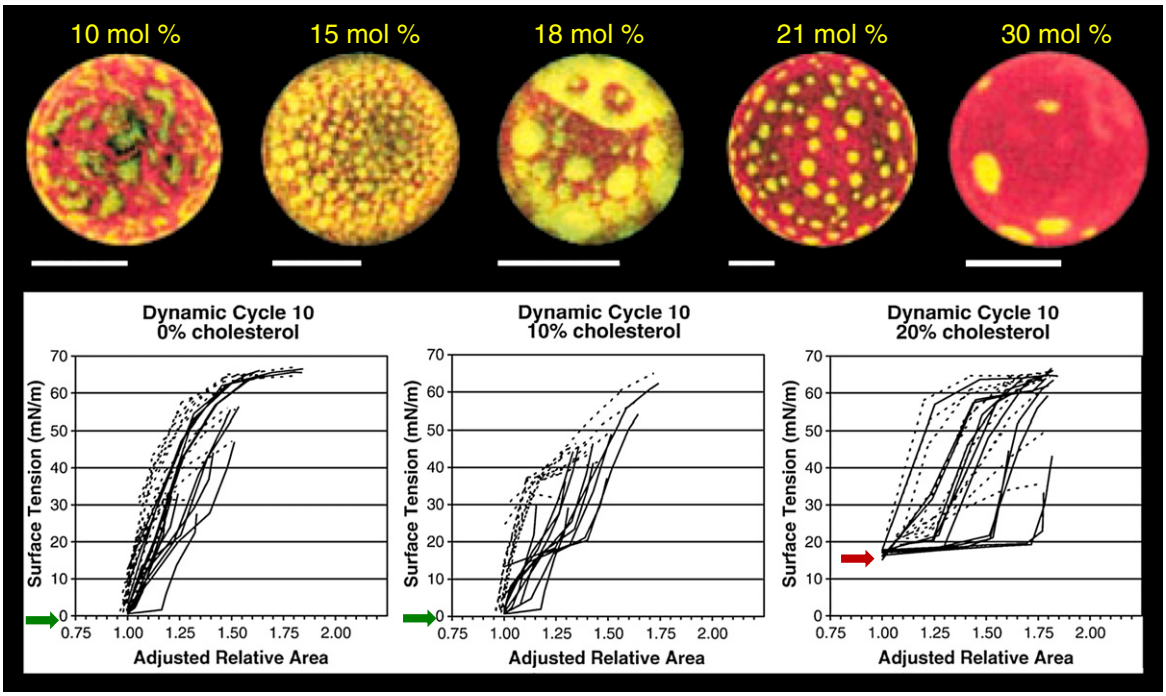

Fig. 8. Cholesterol effects on surfactant phase coexistence and function. Top row: fluorescence images of GUVs from the lipid fraction of porcine surfactant, doped with the fluorescent probes BODIPY-PC and DiIC18, at different cholesterol/PL molar ratios. GUVs formed from surfactant lipid extract with 10 mol% cholesterol show gel/fluid phase coexistence. Increasing the cholesterol concentration to 15 mol% induces the appearance of numerous circular-shaped domains characteristic of L_o/L_d phase coexistence. Further increase in cholesterol (up to 30 mol% relative to PL) yields a significant increase in the area occupied by L_o phase. Images reproduced from [82] with permission. Bottom row: Dynamic cycles of bovine lung surfactant in the absence and presence of different amounts of cholesterol. Samples containing less than 20% cholesterol by mass attain near-zero minimum surface tensions, whereas samples containing 20 wt.% cholesterol only reach surface tensions of 16–20 mN/m.
Adapted from [109] with permission.

attain near-zero surface tensions [109,128–132] and perturb lipid phase coexistence. In this regard, Bernardino de la Serna and co-workers [82] showed that increasing the cholesterol mol% in GUVs composed of surfactant lipids decreases the area covered by the L_d phase in a dose-dependent manner (Fig. 8). In surfactant monolayers, supraphysiological cholesterol levels decrease the area covered by solid-like domains (TC) [111,129]. In addition, AFM studies of bovine lung surfactant films supplemented with 20 wt.% cholesterol indicate that excess cholesterol inhibits the monolayer-to-multilayer transition [110,130,133].

In addition, it has been recently demonstrated that meconium impairs pulmonary surfactant by combined action of cholesterol and bile acids [134]. Micelles of bile acids solubilize cholesterol and facilitate transfer of this sterol to surfactant complexes. Porcine surfactant exposed to meconium showed higher proportions of condensed-like phase domains with a strong tendency to aggregate [134]. It is possible that the probe-excluded domains detected by the authors would correspond to TC and LO phases.

On the other hand, surfactant is also inactivated by incorporation of materials inhaled from the upper airways. For instance, bacterial lipopolysaccharide (LPS), the major component of the outer membrane of Gram negative bacteria, hinders surfactant function. In this regard, our group has determined that LPS incorporation in porcine lipid extract surfactant fluidizes surfactant monolayers and hampers surfactant capability to adsorb to a clean air/water interface and to reduce surface tension to values close to zero (unpublished results). Similar effects have been observed in films of LPS/DPPC mixtures [135,136] and LPS/surfactant-like lipid mixtures [135]. Both smooth LPS [135] and deep rough LPS [136] alter LC/LE phase coexistence in DPPC films, decreasing the size and area coverage of TC domains.

Particle inhalation can also impair surfactant function. In this regard, it has been recently shown that hydroxyapatite nanoparticles (HA-NPs) alter both the function and lateral structure of modified natural surfactant films [137]. On the one hand, HA-NPs exposure reduces adsorption and surface tension-lowering properties of the replacement surfactant Infasurf. On the other hand, HA-NPs decrease the number and size of condensed domains and alter the monolayer-to-multilayer transition [137]. Finally, exposure of surfactant to environmental tobacco smoke (ETS) reduces its surface activity and alters its structure [138]. Surfactant exposed to ETS shows decreased ability to adsorb to the air–water interface and a reduction in the number and size of condensed phase domains [138].

Thus there are several surfactant inhibitors that abolish or reduce ordered/disordered phase coexistence and at the same time interfere with surfactant biophysical functions. Together, these results suggest that pulmonary surfactant is one of the membranous systems in which the coexistence of specialized micrometer-sized membrane domains is required for its function. Entwining of ordered and disordered domains seems to provide a potential mechanism for maintenance of stable interfacial film. A better understanding of surfactant membrane structure, surfactant susceptibility to inhibition, and potential mechanisms to counteract this inhibition is important for the development of new therapies for lung immaturity and chronic inflammatory lung diseases.

Acknowledgements

This work was supported by the Ministerio de Ciencia e Innovación (SAF2009-07810) and Instituto de Salud Carlos III (CIBERES-CB06/06/0002).

References

[1] E.L. Herzog, A.R. Brody, T.V. Colby, R. Mason, M.C. Williams, Knowns and unknowns of the alveolus, Proc. Am. Thorac. Soc. 5 (2008) 778–782.
[2] S. Hawgood, Surfactant: composition, structure, and metabolism, in: R.G. Crystal, J.B. West, P.J. Barnes, E.R. Weibel (Eds.), The Lung: Scientific Foundations, 2nd ed., Lippincott-Raven, Publishers, Philadelphia, 1997, pp. 557–571.

[3] J. Goerke, Pulmonary surfactant: functions and molecular composition, Biochim. Biophys. Acta 1408 (1998) 79–89.
[4] Y.Y. Zuo, R.A. Veldhuizen, A.W. Neumann, N.O. Petersen, F. Possmayer, Current perspectives in pulmonary surfactant—inhibition, enhancement and evaluation, Biochim. Biophys. Acta 1778 (2008) 1947–1977.
[5] J. Pérez-Gil, Structure of pulmonary surfactant membranes and films: the role of proteins and lipid–protein interactions, Biochim. Biophys. Acta 1778 (2008) 1676–1695.
[6] F. Possmayer, S.B. Hall, T. Haller, N.O. Petersen, Y.Y. Zuo, J. Bernardino de la Serna, A.D. Postle, R.A. Veldhuizen, S. Orgeig, Recent advances in alveolar biology: some new looks at the alveolar interface, Respir. Physiol. Neurobiol. 173 (2010) S55–S64.
[7] J.R. Wright, Immunoregulatory functions of surfactant proteins, Nat. Rev. Immunol. 5 (2005) 58–68.
[8] J.A. Whitsett, S.E. Wert, T.E. Weaver, Alveolar surfactant homeostasis and the pathogenesis of pulmonary disease, Annu. Rev. Med. 61 (2010) 105–119.
[9] S. Orgeig, P.S. Hiemstra, E.J. Veldhuizen, C. Casals, H.W. Clark, A. Haczku, L. Knudsen, F. Possmayer, Recent advances in alveolar biology: evolution and function of alveolar proteins, Respir. Physiol. Neurobiol. 173 (2010) S43–S54.
[10] J.A. Whitsett, T.E. Weaver, Hydrophobic surfactant proteins in lung function and disease, N. Engl. J. Med. 347 (2002) 2141–2148.
[11] B. Robertson, H.L. Halliday, Principles of surfactant replacement, Biochim. Biophys. Acta 1408 (1998) 346–361.
[12] A. Günther, C. Ruppert, R. Schmidt, P. Markart, F. Grimminger, D. Walmrath, W. Seeger, Surfactant alteration and replacement in acute respiratory distress syndrome, Respir. Res. 2 (2001) 353–364.
[13] W. Bernhard, J. Mottaghian, A. Gebert, G.A. Rau, H.H. von Der, C.F. Poets, Commercial versus native surfactants. Surface activity, molecular components, and the effect of calcium, Am. J. Respir. Crit. Care Med. 162 (2000) 1524–1533.
[14] M.C. Williams, Conversion of lamellar body membranes into tubular myelin in alveoli of fetal rat lungs, J. Cell Biol. 72 (1977) 260–277.
[15] L.M.G. Van Golde, C. Casals, Metabolism of lipids, in: R.G. Crystal, J.B. West, P.J. Barnes, E.R. Weibel (Eds.), The Lung: Scientific Foundations, 2nd ed., Lippincott-Raven Publishers, Philadelphia, 1997, pp. 9–18.
[16] R. Veldhuizen, K. Nag, S. Orgeig, F. Possmayer, The role of lipids in pulmonary surfactant, Biochim. Biophys. Acta 1408 (1998) 90–108.
[17] A.D. Postle, E.L. Heeley, D.C. Wilton, A comparison of the molecular species compositions of mammalian lung surfactant phospholipids, Comp. Biochem. Physiol. A Mol. Integr. Physiol. 129 (2001) 65–73.
[18] W. Bernhard, S. Hoffmann, H. Dombrowsky, G.A. Rau, A. Kamlage, M. Kappler, J. Haitsma, J. Freihorst, H. von der Hardt, C.F. Poets, Phosphatidylcholine molecular species in lung surfactant: composition in relation to respiratory rate and lung development, Am. J. Respir. Cell Mol. Biol. 25 (2001) 725–731.
[19] X. Jiao, E. Keating, S. Tadayyon, F. Possmayer, Y.Y. Zuo, R.A. Veldhuizen, Atomic force microscopy analysis of rat pulmonary surfactant films, Biophys. Chem. 158 (2011) 119–125.
[20] S. Mukherjee, K. Maiti, M. Fritzen-Garcia, S.C. Bhattacharya, K. Nag, A.K. Panda, S.P. Moulik, Physicochemical studies on goat pulmonary surfactant, Biophys. Chem. 134 (2008) 1–9.
[21] K. Nag, M. Fritzen-Garcia, R. Devraj, A.K. Panda, Interfacial organizations of gel phospholipid and cholesterol in bovine lung surfactant films, Langmuir 23 (2007) 4421–4431.
[22] J. Johansson, T. Curstedt, Molecular structures and interactions of pulmonary surfactant components, Eur. J. Biochem. 244 (1997) 675–693.
[23] S.W. Glasser, A.P. Senft, J.A. Whitsett, M.D. Maxfield, G.F. Ross, T.R. Richardson, D.R. Prows, Y. Xu, T.R. Korfhagen, Macrophage dysfunction and susceptibility to pulmonary *Pseudomonas aeruginosa* infection in surfactant protein C-deficient mice, J. Immunol. 181 (2008) 621–628.
[24] S.W. Glasser, T.L. Witt, A.P. Senft, J.E. Baatz, D. Folger, M.D. Maxfield, H.T. Akinbi, D.A. Newton, D.R. Prows, T.R. Korfhagen, Surfactant protein C-deficient mice are susceptible to respiratory syncytial virus infection, Am. J. Physiol. Lung Cell. Mol. Physiol. 297 (2009) L64–L72.
[25] H. Willander, G. Askarieh, M. Landreh, P. Westermark, K. Nordling, H. Keränen, E. Hermansson, A. Hamvas, L.M. Nogee, T. Bergman, A. Sáenz, C. Casals, J. Åqvist, H. Jörnvall, H. Berglund, J. Presto, S.D. Knight, J. Johansson, High-resolution structure of a BRICHOS domain and its implications for anti-amyloid chaperone activity on lung surfactant protein C, Proc. Natl. Acad. Sci. U. S. A. 109 (2012) 2325–2329.
[26] Y. Wang, P.J. Kuan, C. Xing, J.T. Cronkhite, F. Torres, R.L. Rosenblatt, J.M. DiMaio, L.N. Kinch, N.V. Grishin, C.K. Garcia, Genetic defects in surfactant protein A2 are associated with pulmonary fibrosis and lung cancer, Am. J. Hum. Genet. 84 (2009) 52–59.
[27] J. Johansson, T. Szyperski, T. Curstedt, K. Wuthrich, The NMR structure of the pulmonary surfactant-associated polypeptide SP-C in an apolar solvent contains a valyl-rich alpha-helix, Biochemistry 33 (1994) 6015–6023.
[28] G. Vandenbussche, A. Clercx, T. Curstedt, J. Johansson, H. Jornvall, J.M. Ruysschaert, Structure and orientation of the surfactant-associated protein C in a lipid bilayer, Eur. J. Biochem. 203 (1992) 201–209.
[29] M. Gustafsson, J. Thyberg, J. Näslund, E. Eliasson, J. Johansson, Amyloid fibril formation by pulmonary surfactant protein C, FEBS Lett. 464 (1999) 138–142.
[30] L.M. Gordon, K.Y.C. Lee, A.J. Waring, Conformational mapping of the N-terminal segment of surfactant protein B in lipid using 13C-enhanced Fourier transform infrared spectroscopy, J. Pept. Res. 55 (2000) 330–347.
[31] M. Sarker, A.J. Waring, V. Booth, Structure of mini-B, a functional fragment of surfactant protein B, in detergent micelles, Biochemistry 46 (2007) 11047–11056.
[32] S. Hawgood, M. Derrick, F. Poulain, Structure and properties of surfactant protein B, Biochim. Biophys. Acta 1408 (1998) 150–160.
[33] J. Johansson, T. Curstedt, H. Jörnvall, Surfactant protein B: disulfide bridges, structural properties, and kringle similarities, Biochemistry 30 (1991) 6917–6921.
[34] A. Cruz, C. Casals, I. Plasencia, D. Marsh, J. Perez-Gil, Depth profiles of pulmonary surfactant protein B in phosphatidylcholine bilayers, studied by fluorescence and electron spin resonance spectroscopy, Biochemistry 37 (1998) 9488–9496.
[35] G. Vandenbussche, A. Clercx, M. Clercx, T. Curstedt, J. Johansson, H. Jornvall, J.M. Ruysschaert, Secondary structure and orientation of the surfactant protein SP-B in a lipid environment. A Fourier transform infrared spectroscopy study, Biochemistry 31 (1992) 9169–9176.
[36] D. Schürch, O.L. Ospina, A. Cruz, J. Pérez-Gil, Combined and independent action of proteins SP-B and SP-C in the surface behavior and mechanical stability of pulmonary surfactant films, Biophys. J. 99 (2010) 3290–3299.
[37] C. Casals, I. García-Verdugo, Molecular and functional properties of surfactant protein A, in: K. Nag (Ed.), Developments in Lung Surfactant Dysfunction in Lung Biology in Health and Disease, Marcel Dekker Inc., New York, 2005, pp. 55–84.
[38] F. Sanchez-Barbero, J. Strassner, R. Garcia-Canero, W. Steinhilber, C. Casals, Role of the degree of oligomerization in the structure and function of human surfactant protein A, J. Biol. Chem. 280 (2005) 7659–7670.
[39] J.F. Head, T.R. Mealy, F.X. McCormack, B.A. Seaton, Crystal structure of trimeric carbohydrate recognition and neck domains of surfactant protein A, J. Biol. Chem. 278 (2003) 43254–43260.
[40] K. Håkansson, N.K. Lim, H.J. Hoppe, K.B. Reid, Crystal structure of the trimeric alpha-helical coiled-coil and the three lectin domains of human lung surfactant protein D, Structure 7 (1999) 255–264.
[41] C. Casals, Role of surfactant protein A (SP-A)/lipid interactions for SP-A functions in the lung, Pediatr. Pathol. Mol. Med. 20 (2001) 249–268.
[42] F.X. McCormack, J.A. Whitsett, The pulmonary collectins, SP-A and SP-D, orchestrate innate immunity in the lung, J. Clin. Invest. 109 (2002) 707–712.
[43] P. Dietl, T. Haller, Exocytosis of lung surfactant: from the secretory vesicle to the air–liquid interface, Annu. Rev. Physiol. 67 (2005) 595–621.
[44] T. Haller, P. Dietl, H. Stockner, M. Frick, N. Mair, I. Tinhofer, A. Ritsch, G. Enhorning, G. Putz, Tracing surfactant transformation from cellular release to insertion into an air–liquid interface, Am. J. Physiol. Lung Cell. Mol. Physiol. 286 (2004) L1009–L1015.
[45] C. Bertocchi, A. Ravasio, S. Bernet, G. Putz, P. Dietl, T. Haller, Optical measurement of surface tension in a miniaturized air–liquid interface and its application in lung physiology, Biophys. J. 89 (2005) 1353–1361.
[46] A. Ravasio, B. Olmeda, C. Bertocchi, T. Haller, J. Perez-Gil, Lamellar bodies form solid-three dimensional films at the respiratory air–liquid interface, J. Biol. Chem. 285 (2010) 28174–28182.
[47] S. Schurch, F.H.Y. Green, H. Bachofen, Formation and structure of surface films: captive bubble surfactometry, Biochim. Biophys. Acta 1408 (1998) 180–202.
[48] H. Bachofen, U. Gerber, P. Gehr, M. Amrein, S. Schurch, Structures of pulmonary surfactant films adsorbed to an air–liquid interface in vitro, Biochim. Biophys. Acta 1720 (2005) 59–72.
[49] M. Amrein, A. von Nahmen, M. Sieber, A scanning force- and fluorescence light microscopy study of the structure and function of a model pulmonary surfactant, Eur. Biophys. J. 26 (1997) 349–357.
[50] R.V. Diemel, M.M. Snel, A.J. Waring, F.J. Walther, L.M. van Golde, G. Putz, H.P. Haagsman, J.J. Batenburg, Multilayer formation upon compression of surfactant monolayers depends on protein concentration as well as lipid composition. An atomic force microscopy study, J. Biol. Chem. 277 (2002) 21179–21188.
[51] D. Follows, F. Tiberg, R.K. Thomas, M. Larsson, Multilayers at the surface of solutions of exogenous lung surfactant: direct observation by neutron reflection, Biochim. Biophys. Acta 1768 (2007) 228–235.
[52] S. Schurch, R. Qanbar, H. Bachofen, F. Possmayer, The surface-associated surfactant reservoir in the alveolar lining, Biol. Neonate 67 (1995) 61–76.
[53] S. Baoukina, D.P. Tieleman, Lung surfactant protein SP-B promotes formation of bilayer reservoirs from monolayer and lipid transfer between the interface and subphase, Biophys. J. 100 (2011) 1678–1687.
[54] M. Chavarha, H. Khoojinian, L.E. Jr Schulwitz, S.C. Biswas, S.B. Rananavare, S.B. Hall, Hydrophobic surfactant proteins induce a phosphatidylethanolamine to form cubic phases, Biophys. J. 98 (2010) 1549–1557.
[55] R.S. Farver, F.D. Mills, V.C. Antharam, J.N. Chebukati, G.E. Fanucci, J.R. Long, Lipid polymorphism induced by surfactant peptide SP-B(1–25), Biophys. J. 99 (2010) 1773–1782.
[56] Y. Suzuki, Y. Fujita, K. Kogishi, Reconstitution of tubular myelin from synthetic lipids and proteins associated with pig pulmonary surfactant, Am. Rev. Respir. Dis. 140 (1989) 75–81.
[57] T.R. Korfhagen, A.M. LeVine, J.A. Whitsett, Surfactant protein A (SP-A) gene targeted mice, Biochim. Biophys. Acta 1408 (1998) 296–302.
[58] E. Putman, L.A. Creuwels, L.M. van Golde, H.P. Haagsman, Surface properties, morphology and protein composition of pulmonary surfactant subtypes, Biochem. J. 320 (1996) 599–605.
[59] R. Veldhuizen, F. Possmayer, Phospholipid metabolism in lung surfactant, Subcell. Biochem. 37 (2004) 359–388.
[60] D. Chapman, Phase transitions and fluidity characteristics of lipids and cell membranes, Q. Rev. Biophys. 8 (1975) 185–235.
[61] D.R. Silvius, Thermotropic Phase Transitions of Pure Lipids in Model Membranes and Their Modifications by Membrane Proteins, John Wiley & Sons Inc., New York, 1982.
[62] T. Heimburg, A model for the lipid pretransition: coupling of ripple formation with the chain-melting transition, Biophys. J. 78 (2000) 1154–1165.
[63] C.D. Stubbs, Membrane fluidity: structure and dynamics of membrane lipids, Essays Biochem. 19 (1983) 1–39.
[64] J.F. Tocanne, L. Dupou-Cézanne, A. Lopez, Lateral diffusion of lipids in model and natural membranes, Prog. Lipid Res. 33 (1994) 203–237.
[65] N. Yellin, I.W. Levin, Hydrocarbon trans-gauche isomerization in phospholipid bilayer gel assemblies, Biochemistry 16 (1977) 642–647.

[66] B.R. Lentz, D.A. Barrow, M. Hoechli, Cholesterol–phosphatidylcholine interactions in multilamellar vesicles, Biochemistry 19 (1980) 1943–1954.
[67] O.G. Mouritsen, M.J. Zuckermann, What's so special about cholesterol? Lipids 39 (2004) 1101–1113.
[68] P.J. Quinn, C. Wolf, The liquid-ordered phase in membranes, Biochim. Biophys. Acta 1788 (2009) 33–46.
[69] O.G. Mouritsen, The liquid-ordered state comes of age, Biochim. Biophys. Acta 1798 (2010) 1286–1288.
[70] S. Orgeig, C.B. Daniels, The roles of cholesterol in pulmonary surfactant: insights from comparative and evolutionary studies, Comp. Biochem. Physiol. A Mol. Integr. Physiol. 129 (2001) 75–89.
[71] W. Stillwell, T. Dallman, A.C. Dumaual, F.T. Crump, L.J. Jenski, Cholesterol versus alpha-tocopherol: effects on properties of bilayers made from heteroacid phosphatidylcholines, Biochemistry 35 (1996) 13353–13362.
[72] M.R. Vist, J.H. Davis, Phase equilibria of cholesterol/dipalmitoylphosphatidylcholine mixtures: 2H nuclear magnetic resonance and differential scanning calorimetry, Biochemistry 29 (1990) 451–464.
[73] S.L. Veatch, S.L. Keller, Seeing spots: complex phase behavior in simple membranes, Biochim. Biophys. Acta 1746 (2005) 172–185.
[74] A. Sáenz, O. Cañadas, L.A. Bagatolli, M.E. Johnson, C. Casals, Physical properties and surface activity of surfactant-like membranes containing the cationic and hydrophobic peptide KL4, FEBS J. 273 (2006) 2515–2527.
[75] R. Wustneck, J. Perez-Gil, N. Wustneck, A. Cruz, V.B. Fainerman, U. Pison, Interfacial properties of pulmonary surfactant layers, Adv. Colloid Interface Sci. 117 (2005) 33–58.
[76] K. Nag, C. Boland, N. Rich, K.M. Keough, Epifluorescence microscopic observation of monolayers of dipalmitoylphosphatidylcholine: dependence of domain size on compression rates, Biochim. Biophys. Acta 1068 (1991) 157–160.
[77] O. Cañadas, R. Guerrero, R. García-Cañero, G. Orellana, M. Menéndez, C. Casals, Characterization of liposomal tacrolimus in lung surfactant-like phospholipids and evaluation of its immunosuppressive activity, Biochemistry 43 (2004) 9926–9938.
[78] S.L. Duncan, I.S. Dalal, R.G. Larson, Molecular dynamics simulation of phase transitions in model lung surfactant monolayers, Biochim. Biophys. Acta 1808 (2011) 2450–2465.
[79] H. Zhang, Q. Fan, Y.E. Wang, C.R. Neal, Y.Y. Zuo, Comparative study of clinical pulmonary surfactants using atomic force microscopy, Biochim. Biophys. Acta 1808 (2011) 1832–1842.
[80] H. Zhang, Y.E. Wang, Q. Fan, Y.Y. Zuo, On the low surface tension of lung surfactant, Langmuir 27 (2011) 8351–8358.
[81] E. Keating, Y.Y. Zuo, S.M. Tadayyon, N.O. Petersen, F. Possmayer, R.A.W. Veldhuizen, A modified squeeze-out mechanism for generating high surface pressures with pulmonary surfactant, Biochim. Biophys. Acta 1818 (2012) 1225–1234.
[82] J. Bernardino de la Serna, J. Perez-Gil, A.C. Simonsen, L.A. Bagatolli, Cholesterol rules: direct observation of the coexistence of two fluid phases in native pulmonary surfactant membranes at physiological temperatures, J. Biol. Chem. 279 (2004) 40715–40722.
[83] J. Bernardino de la Serna, G. Orädd, L.A. Bagatolli, A.C. Simonsen, D. Marsh, G. Lindblom, J. Perez-Gil, Segregated phases in pulmonary surfactant membranes do not show coexistence of lipid populations with differentiated dynamic properties, Biophys. J. 97 (2009) 1381–1389.
[84] A. Sáenz, A. López-Sánchez, J. Mojica-Lázaro, L. Marínez-Caro, N. Nin, L.A. Bagatolli, C. Casals, Fluidizing effects of C-reactive protein on lung surfactant membranes: protective role of surfactant protein A, FASEB J. 24 (2010) 3662–3673.
[85] A. Sáenz, O. Cañadas, L.A. Bagatolli, F. Sánchez-Barbero, M.E. Johnson, C. Casals, Effect of surfactant protein A on the physical properties and surface activity of KL4-surfactant, Biophys. J. 92 (2007) 482–492.
[86] K. Nag, J.S. Pao, R.R. Harbottle, F. Possmayer, N.O. Petersen, L.A. Bagatolli, Segregation of saturates chain lipids in pulmonary surfactant films and bilayers, Biophys. J. 82 (2002) 2041–2051.
[87] Y.Y. Zuo, E. Keating, L. Zhao, S.M. Tadayyon, R.A. Veldhuizen, N.O. Petersen, F. Possmayer, Atomic force microscopy studies of functional and dysfunctional pulmonary surfactant films. I. Micro- and nanostructures of functional pulmonary surfactant films and the effect of SP-A, Biophys. J. 94 (2008) 3549–3564.
[88] Y.Y. Zuo, S.M. Tadayyon, E. Keating, L. Zhao, R.A. Veldhuizen, N.O. Petersen, M.W. Amrein, F. Possmayer, Atomic force microscopy studies of functional and dysfunctional pulmonary surfactant films, II: albumin-inhibited pulmonary surfactant films and the effect of SP-A, Biophys. J. 95 (2008) 2779–2791.
[89] E. Keating, A.J. Waring, F.J. Walther, F. Possmayer, R.A. Veldhuizen, N.O. Petersen, A ToF-SIMS study of the lateral organization of lipids and proteins in pulmonary surfactant systems, Biochim. Biophys. Acta 1808 (2011) 614–621.
[90] M. Saleem, H.J. Galla, Surface view of the lateral organization of lipids and proteins in lung surfactant model systems—a ToF-SIMS approach, Biochim. Biophys. Acta 1798 (2010) 730–740.
[91] K. Nag, J. Perez-Gil, M.L.F. Ruano, L.A.D. Worthman, J. Stewart, C. Casals, K.M.W. Keough, Phase transitions in films of lung surfactant at the air–water interface, Biophys. J. 74 (1998) 2983–2995.
[92] L.A. Worthman, K. Nag, N. Rich, M.L. Ruano, C. Casals, J. Perez-Gil, K.M. Keough, Pulmonary surfactant protein A interacts with gel-like regions in monolayers of pulmonary surfactant lipid extract, Biophys. J. 79 (2001) 2657–2666.
[93] B.M. Discher, K.M. Maloney, W.R. Schief Jr., D.W. Grainger, V. Vogel, S.B. Hall, Lateral phase separation in interfacial films of pulmonary surfactant, Biophys. J. 71 (1996) 2583–2590.
[94] B.M. Discher, K.M. Maloney, D.W. Grainger, C.A. Sousa, S.B. Hall, Neutral lipids induce critical behavior in interfacial monolayers of pulmonary surfactant, Biochemistry 38 (1999) 374–383.
[95] B.M. Discher, W.R. Schief, V. Vogel, S.B. Hall, Phase separation in monolayers of pulmonary surfactant phospholipids at the air–water interface: composition and structure, Biophys. J. 77 (1999) 2051–2061.
[96] B. Piknova, W.R. Schief, V. Vogel, S.B. Hall, Discrepancy between phase behavior of lung surfactant phospholipids and the classical model of surfactant function, Biophys. J. 81 (2001) 2172–2180.
[97] A. von Nahmen, M. Schenk, M. Sieber, M. Amrein, The structure of a model pulmonary surfactant as revealed by scanning force microscopy, Biophys. J. 72 (1997) 463–469.
[98] N. Bourdos, F. Kollmer, A. Benninghoven, M. Ross, M. Sieber, H.J. Galla, Analysis of lung surfactant model systems with time-of-flight secondary ion mass spectrometry, Biophys. J. 79 (2000) 357–369.
[99] A. Cruz, L. Vázquez, M. Vélez, J. Pérez-Gil, Effect of pulmonary surfactant protein SP-B on the micro- and nanostructure of phospholipid films, Biophys. J. 86 (2004) 308–320.
[100] K. Nag, S.G. Taneva, J. Perez-Gil, A. Cruz, K.M. Keough, Combinations of fluorescently labeled pulmonary surfactant proteins SP-B and SP-C in phospholipid films, Biophys. J. 72 (1997) 2638–2650.
[101] K. Nag, J. Perez-Gil, A. Cruz, K.M. Keough, Fluorescently labeled pulmonary surfactant protein C in spread phospholipid monolayers, Biophys. J. 71 (1996) 246–256.
[102] A. Kramer, A. Wintergalen, M. Sieber, H.J. Galla, M. Amrein, R. Guckenberger, Distribution of the surfactant-associated protein C within a lung surfactant model film investigated by near-field optical microscopy, Biophys. J. 78 (2000) 458–465.
[103] M. Seifert, D. Breitenstein, U. Klenz, M.C. Meyer, H.J. Galla, Solubility versus electrostatics: what determines lipid/protein interaction in lung surfactant, Biophys. J. 93 (2007) 1192–1203.
[104] S. Krol, M. Ross, M. Sieber, S. Kunneke, H.-J. Galla, A. Janshoff, Formation of three-dimensional protein-lipid aggregates in monolayer films induced by surfactant protein B, Biophys. J. 79 (2000) 904–918.
[105] M.L.F. Ruano, N. Kaushik, L. Worthman, C. Casals, J. Pérez-Gil, K.M.W. Keough, Differential partitioning of pulmonary surfactant protein SP-A into regions of monalayers of dipalmitoylphosphatidylcholine (DPPC) and DPPC/dipalmitoylphosphatidylglycerol, Biophys. J. 74 (1998) 1101–1109.
[106] M.L.F. Ruano, N. Nag, C. Casals, J. Pérez-Gil, K.M.W. Keough, Interactions of pulmonary surfactant protein A with phospholipid monolayers change with pH, Biophys. J. 77 (1999) 1469–1476.
[107] F. Sanchez-Barbero, G. Rivas, W. Steinhilber, C. Casals, Structural and functional differences among human surfactant proteins SP-A1, SP-A2, and coexpressed SP-A1/SP-A2. Role of supratrimeric oligomerization, Biochem. J. 406 (2007) 479–489.
[108] I. García-Verdugo, G. Guirong, J. Floros, C. Casals, Structural analysis and lipid binding properties of recombinant human surfactant protein A (SP-A) derived from one (SP-A1 or SP-A2) or both genes, Biochemistry 41 (2002) 14041–14053.
[109] L. Gunasekara, S. Schurch, W.M. Schoel, K. Nag, Z. Leonenko, M. Haufs, M. Amrein, Pulmonary surfactant function is abolished by an elevated proportion of cholesterol, Biochim. Biophys. Acta, Mol. Cell Biol. Lipids 1737 (2005) 27–35.
[110] Z. Leonenko, S. Gill, S. Baoukina, L. Monticelli, J. Doehner, L. Gunasekara, F. Felderer, M. Rodenstein, L.M. Eng, M.W. Amrein, An elevated level of cholesterol impairs self assembly of pulmonary surfactant into a functional film, Biophys. J. 93 (2007) 674–683.
[111] S. Malcharek, A. Hinz, L. Hilterhaus, H.J. Galla, Multilayer structures in lipid monolayer films containing surfactant protein C: effects of cholesterol and POPE, Biophys. J. 88 (2005) 2638–2649.
[112] S. Baoukina, L. Monticelli, M. Amrein, D.P. Tieleman, The molecular mechanism of monolayer–bilayer transformations of lung surfactant from molecular dynamics simulations, Biophys. J. 93 (2007) 3775–3782.
[113] M.M. Lipp, K.Y.C. Lee, D.Y. Takamoto, J.A. Zasadzinski, A.J. Waring, Coexistence of buckled and flat monolayers, Phys. Rev. Lett. 81 (1998) 1650–1653.
[114] A. von Nahmen, A. Post, H.J. Galla, M. Sieber, The phase behavior of lipid monolayers containing pulmonary surfactant protein C studied by fluorescence light microscopy, Eur. Biophys. J. 26 (1997) 359–369.
[115] F. Hane, B. Moores, M. Amrein, Z. Leonenko, Effect of SP-C on surface potential distribution in pulmonary surfactant: atomic force microscopy and Kelvin probe force microscopy study, Ultramicroscopy 109 (2009) 968–973.
[116] H.J. Galla, N. Bourdos, A. von Nahmen, M. Amrein, M. Sieber, The role of pulmonary surfactant protein C during the breathing cycle, Thin Solid Films 327–329 (1998) 632–635.
[117] L.A. Creuwels, E.H. Boer, R.A. Demel, L.M. van Golde, H.P. Haagsman, Neutralization of the positive charges of surfactant protein C. Effects on structure and function, J. Biol. Chem. 270 (1995) 16225–16229.
[118] S. Baoukina, D.P. Tieleman, Direct simulation of protein-mediated vesicle fusion: lung surfactant protein B, Biophys. J. 99 (2010) 2134–2142.
[119] M. Ross, S. Krol, A. Janshoff, H.J. Galla, Kinetics of phospholipid insertion into monolayers containing the lung surfactant proteins SP-B or SP-C, Eur. Biophys. J. 31 (2002) 52–61.
[120] M.A. Oosterlanden-Dijksterhuis, H.P. Haagsman, L.M. van Golde, R.A. Demel, Characterization of lipid insertion into monomolecular layers mediated by lung surfactant proteins SP-B and SP-C, Biochemistry 30 (1991) 10965–10971.
[121] A. Saenz, L. Alvarez, M. Santos, A. Lopez-Sanchez, J.L. Castillo-Olivares, A. Varela, R. Segal, C. Casals, Beneficial effects of synthetic KL4-surfactant in experimental lung transplantation, Eur. Respir. J. 37 (2011) 925–932.

[122] C. Casals, A. Varela, M.L. Ruano, F. Valino, J. Perez-Gil, N. Torre, E. Jorge, F. Tendillo, J.L. Castillo-Olivares, Increase of C-reactive protein and decrease of surfactant protein A in surfactant after lung transplantation, Am. J. Respir. Crit. Care Med. 157 (1998) 43–49.
[123] J.J. Li, R.L. Sanders, K.P. McAdam, C.A. Hales, B.T. Thompson, J.A. Gelfand, J.F. Burke, Impact of C-reactive protein (CRP) on surfactant function, J. Trauma 29 (1989) 1690–1697.
[124] K. Nag, K. Rodriguez-Capote, A.K. Panda, L. Frederik, S.A. Hearn, N.O. Petersen, S. Schürch, F. Possmayer, Disparate effects of two phosphatidylcholine binding proteins, C-reactive protein and surfactant protein A, on pulmonary surfactant structure and function, Am. J. Physiol. Lung Cell. Mol. Physiol. 287 (2004) L1145–L1153.
[125] J.D. Amirkhanian, H.W. Taeusch, Reversible and irreversible inactivation of preformed pulmonary surfactant surface films by changes in subphase constituents, Biochim. Biophys. Acta 1165 (1993) 321–326.
[126] T.M. McEachren, K.M. Keough, Phosphocholine reverses inhibition of pulmonary surfactant adsorption caused by C-reactive protein, Am. J. Physiol. 269 (1995) L492–L497.
[127] K. Nag, S. Vidyashankar, R. Devraj, M. Fritzen Garcia, A.K. Panda, Physicochemical studies on the interaction of serum albumin with pulmonary surfactant extract in films and bulk bilayer phase, J. Colloid Interface Sci. 352 (2010) 456–464.
[128] L. Gunasekara, W.M. Schoel, S. Schürch, M.W. Amrein, A comparative study of mechanisms of surfactant inhibition, Biochim. Biophys. Acta 1778 (2008) 433–444.
[129] A.K. Panda, K. Nag, R.R. Harbottle, K. Rodriguez-Capote, R.A. Veldhuizen, N.O. Petersen, F. Possmayer, Effect of acute lung injury on structure and function of pulmonary surfactant films, Am. J. Respir. Cell Mol. Biol. 30 (2004) 641–650.
[130] E. Keating, L. Rahman, J. Francis, A. Petersen, F. Possmayer, R. Veldhuizen, N.O. Petersen, Effect of cholesterol on the biophysical and physiological properties of a clinical pulmonary surfactant, Biophys. J. 93 (2007) 1391–1401.
[131] F. Hane, E. Drolle, Z. Leonenko, Effect of cholesterol and amyloid-β peptide on structure and function of mixed-lipid films and pulmonary surfactant BLES: an atomic force microscopy study, Nanomedicine 6 (2010) 808–814.
[132] D. Vockeroth, L. Gunasekara, M. Amrein, F. Possmayer, J.F. Lewis, R.A. Veldhuizen, Role of cholesterol in the biophysical dysfunction of surfactant in ventilator-induced lung injury, Am. J. Physiol. Lung Cell. Mol. Physiol. 298 (2010) L117–L125.
[133] E. Finot, Y. Leonenko, B. Moores, L. Eng, M. Amrein, Z. Leonenko, Effect of cholesterol on electrostatics in lipid-protein films of a pulmonary surfactant, Langmuir 26 (2010) 1929–1935.
[134] E. Lopez-Rodriguez, M. Echaide, A. Cruz, H.W. Taeusch, J. Perez-Gil, Meconium impairs pulmonary surfactant by a combined action of cholesterol and bile acids, Biophys. J. 100 (2011) 646–655.
[135] O. Cañadas, K.M. Keough, C. Casals, Bacterial lipopolysaccharide promotes destabilization of lung surfactant-like films, Biophys. J. 100 (2011) 108–116.
[136] I. Garcia-Verdugo, O. Cañadas, S.G. Taneva, K.M. Keough, C. Casals Surfactant, Protein A forms extensive lattice-like structures on 1,2-dipalmitoylphosphatidylcholine/rough-lipopolysaccharide-mixed monolayers, Biophys. J. 93 (2007) 3529–3540.
[137] Q. Fan, Y.E. Wang, X. Zhao, J.S. Loo, Y.Y. Zuo Adverse, Biophysical effects of hydroxyapatite nanoparticles on natural pulmonary surfactant, ACS Nano 5 (2011) 6410–6416.
[138] P.C. Stenger, C. Alonso, J.A. Zasadzinski, A.J. Waring, C.L. Jung, K.E. Pinkerton, Environmental tobacco smoke effects on lung surfactant film organization, Biochim. Biophys. Acta 1788 (2009) 358–370.